

Electronic Supplementary Information (ESI) for

Crosslinked Cyanometallate-Chitosan Nanosheet Assembled Aerogels as Efficient Catalysts to Boost Polysulfide Redox Kinetics in Lithium-Sulfur Batteries

Zhongsong Fang,^{§a} Xuanhe Hu,^{§a} Chenhao Shu,^{§a} Junhua Jian,^a Jie Liu,^a and Dingshan Yu^{*a}

Z. Fang,^{§a} X. Hu,^{§a} C. Shu,^{§a} J. Jian,^a J. Liu,^a and Prof. D. S. Yu^{*a}

^aKey Laboratory for Polymeric Composite and Functional Materials of Ministry of Education,
Key Laboratory of High Performance Polymer-based Composites of Guangdong Province
School of Chemistry
Sun Yat-Sen University
Guangzhou, 510275, P. R. China
E-mail: yudings@mail.sysu.edu.cn.

Experimental Section

Preparation of Fe-CS: 2 mL of $K_3Fe(CN)_6$ (KFCN, Tianjin Fuchen Chemical Reagents Factory) aqueous solution (0.5 mol L^{-1}) was mixed with 20 mL of chitosan (10 mg mL^{-1} , Shanghai Yuanye Bio-Technology Co., Ltd) in acid solution ($0.5 \text{ wt } \%$, Guangzhou Chemical Reagent Factory) at room temperature. After ultrasonication for 5 min, the yellow hydrogel was obtained. Subsequently, the hydrogel was putted into the dialysis bag and washed with plenty of deionized water to remove impurities and then freeze-dried for 24 h to obtain Fe-CS (C 56.29 at %, O 26.00 at %, N 15.39 at %, K 0.58 at %, Fe 1.74 at % from XPS; C 41.79 wt %, O 23.16 wt %, N 19.35 wt %, K 0.04 wt %, Fe 15.67 wt % from SEM-EDX). Co-CS was also prepared via the similar procedure where KFCN was replaced by $K_3Co(CN)_6$ (Shanghai Aladdin Biochemical Technology Co., Ltd).

Preparation of Fe-CS/CB Modified Separator: The obtained Fe-CS, carbon black (CB, Lion Co.), and poly(vinylidene difluoride) (PVDF, Arkema Inc.) were mixed at a weight of 90, 180 and 30 mg in N-methyl-pyrrolidone (NMP, Shanghai Aladdin Biochemical Technology Co., Ltd), and the slurry was coated onto the Celgard 2400 separator. Then, the modified separator was dried at $60 \text{ }^\circ\text{C}$ for 24 h and cut into circular disks with the diameter of 16 mm. CB, CS/CB, KFCN/CB and Co-CS/CB modified separator were prepared by the similar process.

Visualized Adsorption: The Li_2S_6 solution was prepared by mixing lithium sulfide (Li_2S , Alfa Aesar Co., Ltd) and sulfur (DK Nano technology) in a molar ratio of 1:5 in 1, 2-dimethoxyethane (DME, Shanghai Aladdin Biochemical Technology Co., Ltd) with vigorous stirring at $70 \text{ }^\circ\text{C}$ for 24 h. Different adsorbents with the same weight of 15 mg were added to 2 mL above Li_2S_6 solution, respectively. After stewing for 24 h, the digital photograph and corresponding UV-vis spectra were taken and measured, respectively.

Assembly of Li_2S_6 - Li_2S_6 Symmetric Cells: Two pieces of carbon cloth as the electrodes were assembled into CR2032 coin cells with different modified separators. 60 μL 1, 3-dioxolane (DOL)/DME (v/v=1/1) electrolyte (Nanjing MJS Energy Technology) containing 0.2 mol L^{-1} Li_2S_6 , 1 mol L^{-1} bis (trifluoromethanesulfonyl) imide (LiTFSI), and 1.0 wt % LiNO_3 was used. The cyclic voltammograms (CV) curve of symmetric cell was obtained at a scan rate of 50 mV s^{-1} within a voltage window of -0.8-0.8 V. The corresponding current of different symmetric cells is recorded based on the same weight of the separator modification material.

Nucleation Measurement: Nucleation of Li_2S was tested in CR2032 coin cells, where 30 μL Li_2S_8 tetraglyme solution (Nanjing MJS Energy Technology) with 2.0 mol L^{-1} [S] and 1.0 mol L^{-1} LiTFSI dropped onto the carbon cloth served as cathode, a piece of lithium foil worked as the anode, and 30 μL blank electrolyte without Li_2S_8 was used as the anolyte. The cells with modified separators were first galvanostatically discharged at 0.112 mA to 2.06 V, and kept at 2.05 V potentiostatically with a terminated current of 10^{-5} A. Faraday's law was used to calculate the capacity of deposited lithium sulfide.^[1]

Preparation of Sulfur Cathodes: Simple carbon/sulfur composite as the cathode was prepared by mixing ketjen black (100 mg) and sulfur powder (200 mg) with a mass ratio of 1:2. The obtained mixture was further stirred with the PVDF binder (33.3 mg) at a mass ratio of 9:1 in NMP to form a homogeneous slurry. Then, the slurry was coated on the carbon coated aluminum foil by a doctor blade and dried at 60 $^\circ\text{C}$ for 24 h. The electrodes were cut into discs with a sulfur loading of $\sim 1.5 \text{ mg cm}^{-2}$. The cathodes with high sulfur loading were fabricated by similar process, while carbon cloth was applied as current collector.

Characterization: The morphologies of the samples were characterized by scanning

electron microscopy (SEM, S4800) and transmission electron microscopy (TEM, JEOL JEM-2100). X-ray diffraction (XRD) patterns were measured on a Rigaku SmartLab under Cu K α radiation ($\lambda = 1.54056 \text{ \AA}$) operated at 40 kV and 30 mA with a scanning rate of $10^\circ \text{ min}^{-1}$. The Fourier transform infrared (FT-IR) measurements were performed on a Nexus 670 spectrograph. The surface chemistry was analyzed by X-ray photoelectron spectroscopy (XPS, ESCALAB 250). Polysulfides adsorption was measured by UV-vis spectroscopy (PerkinElmer). The surface area was determined by the Brunauer-Emmett-Teller (BET) method on an ASAP 2460 system.

Electrochemical Measurements: Coin cells (CR2032) were assembled with lithium foil as the anode. The electrolyte (Shanghai Song Jing Energy Technology Co., Ltd) was 1.0 mol L^{-1} LiTFSI dissolved in DOL/DME (v/v = 1:1) with 1.0 wt % LiNO $_3$ as the additive. The amount of electrolyte used in normal sulfur loading and high sulfur loading cells were controlled with the electrolyte/sulfur (E/S) ratio of 12 and $10 \mu\text{L mg}^{-1}$, respectively. CV measurements were carried out with a scanning rate of 0.1 mV s^{-1} . EIS was tested from 0.1 to 100 kHz (Autolab PGSTAT 302N). Galvanostatic charge-discharge test was performed within a voltage window of 1.7-2.8 V at room temperature (LAND CT2001A).

Theoretical calculations: Density functional theory (DFT) calculations were conducted by using the DMol3 package in Materials Studio of Accelrys Inc. The generalized gradient approximation (GGA) employing Perdew-Burke-Ernzerhof (PBE) functional and all-electron double numerical plus polarization (DNP) basis set were used. The DFT-D method was performed to correct for the van der Waals (vdW) interactions when the adsorption of polysulfides is considered. The convergence tolerances were set to the displacement of 5.0×10^{-3}

Å, the force of $2.0 \times 10^{-3} \text{ Ha } \text{Å}^{-1}$, and the energy change of $1.0 \times 10^{-5} \text{ Ha}$. Ha, a symbol of hartree, is the atomic unit of energy. $1 \text{ Ha} = 4.360 \times 10^{-18} \text{ J} = 27.21 \text{ eV}$.

The geometries of $\text{K}_3\text{Fe}(\text{CN})_6$ crystals, chitosan and cyanometalate-chitosan were firstly optimized. The binding energy E_b between Li_2S_6 and the above three materials was calculated as follows:

$$E_b = E_{total} - E_M - E_{Li_2S_6}$$

Where E_M , $E_{Li_2S_6}$, E_{total} are the energies of the three different materials, an isolated Li_2S_6 molecule and Li_2S_6 adsorbed on the three slabs, respectively. Higher binding energy represents stronger interaction.

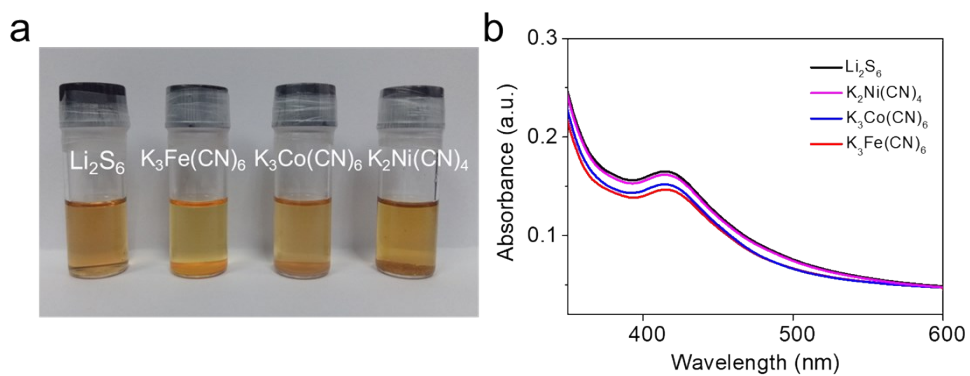


Fig. S1 (a) Static adsorption of Li_2S_6 by different cyanometalates. (b) Corresponding UV-vis spectra.

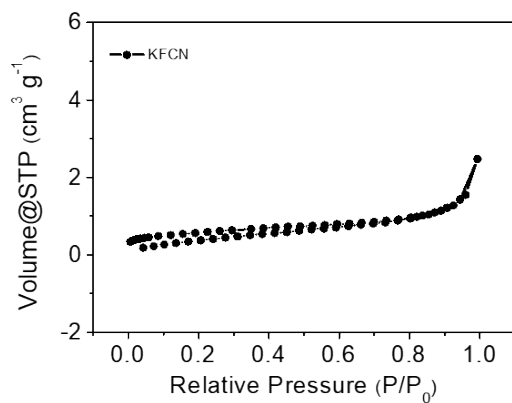


Fig. S2 N_2 absorption and desorption isotherms of KFCN.



Fig. S3 Photograph of CS aqueous solution and KFCN cross-linked chitosan hydrogel.

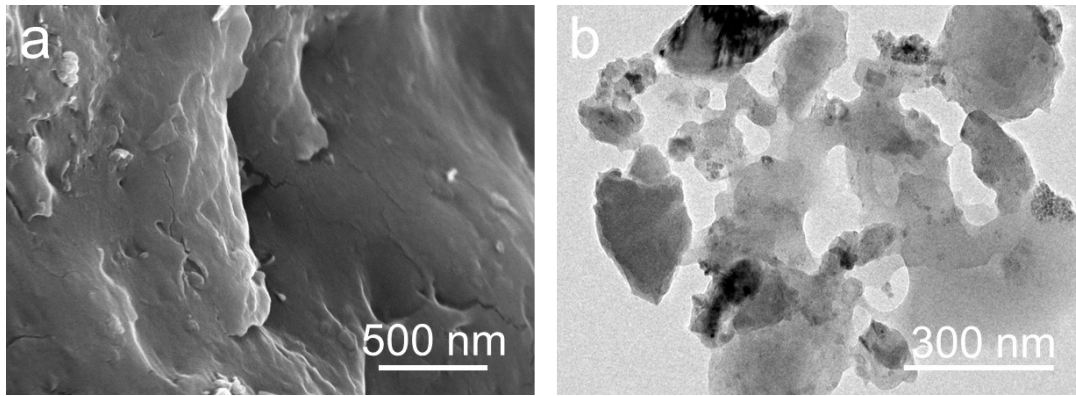


Fig. S4. (a) SEM and (b) TEM images of pristine chitosan.

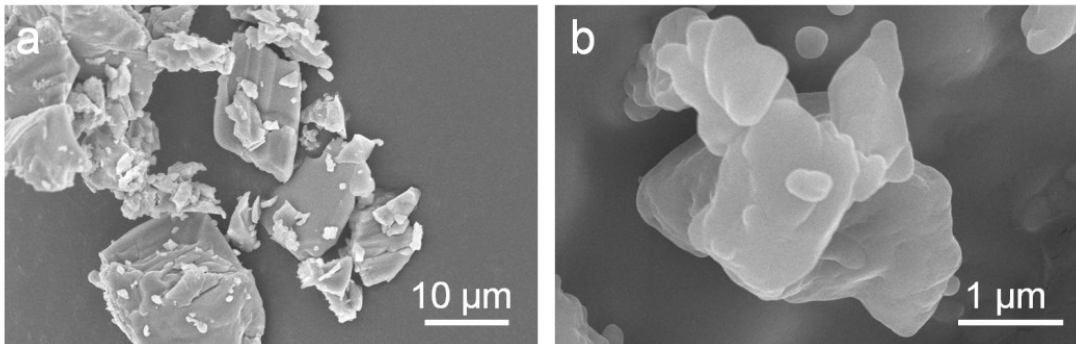


Fig. S5 SEM images of KFCN particles.

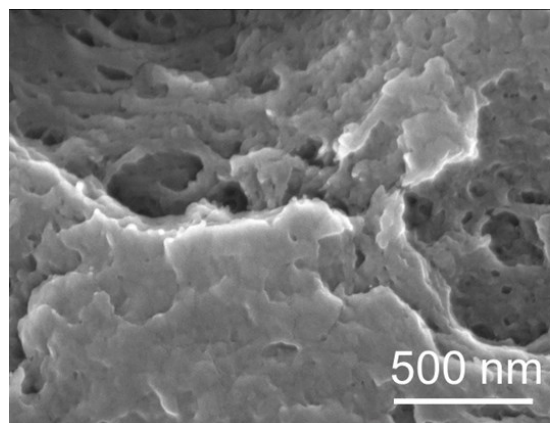


Fig. S6. SEM image of Fe-CS.

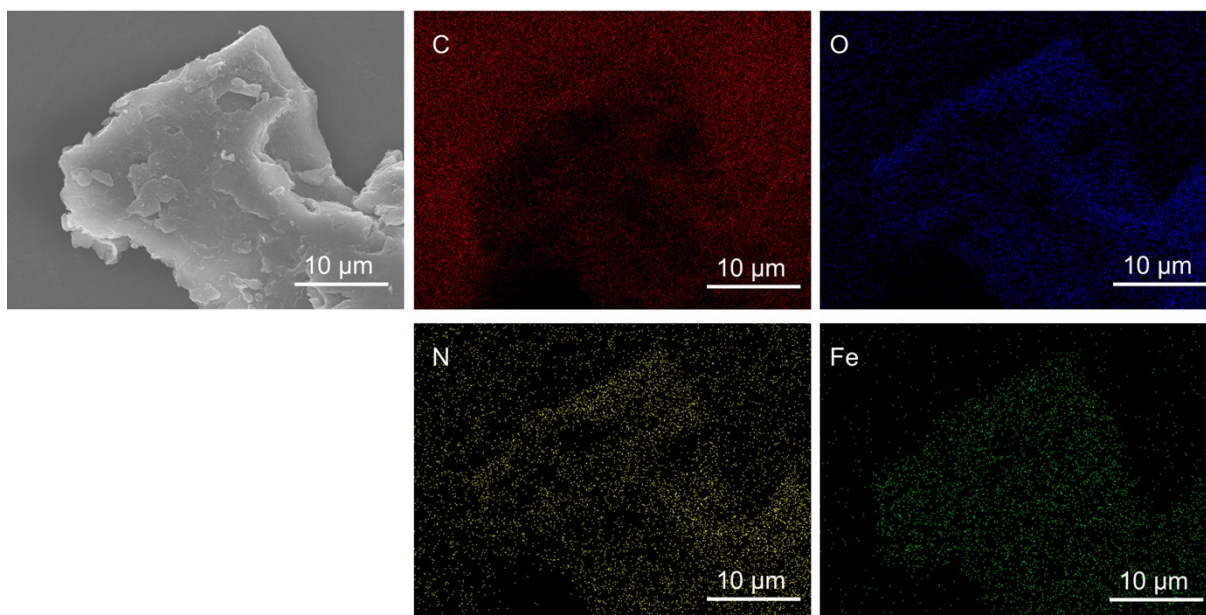


Fig. S7 SEM image and corresponding elemental mappings of Fe-CS.

It is noted that the sample is put on a conductive substrate (conductive adhesive) for EDX analysis, which contains many C elements. The difference of C and Fe mapping compared with N and O mapping can be explained that the C elements from the substrate exert an influence on the C mapping while the content of Fe element in Fe-CS gel is rather low. N and O mapping are halfway since the contents of these two elements is enough high and the substrate has a negligible influence on them. Similar case was observed in previous study.^[2]

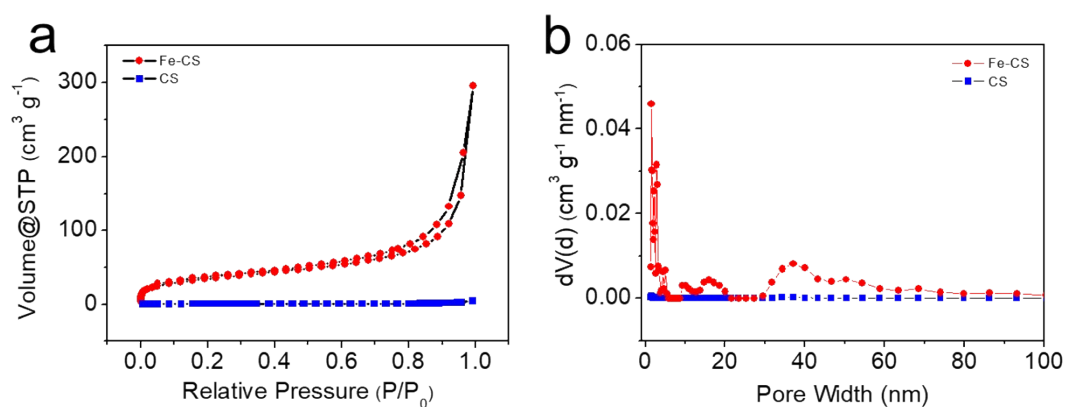


Fig. S8 (a) N_2 adsorption and desorption isotherms and (b) pore-size distributions curves of Fe-CS and CS.

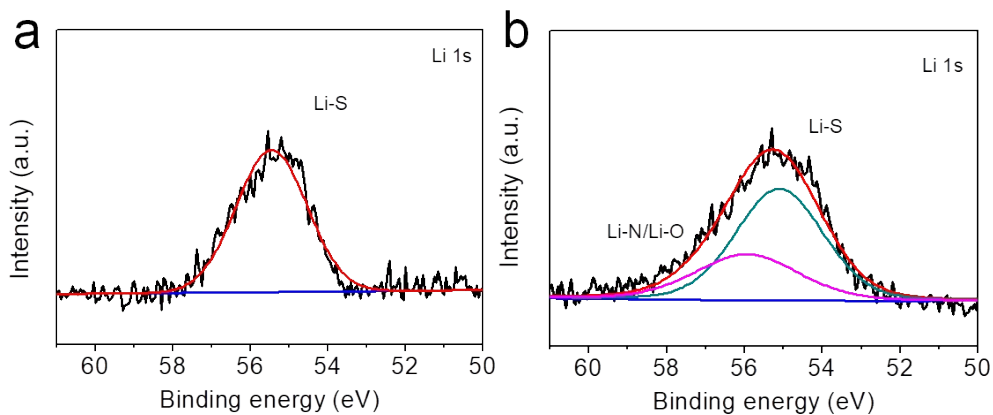


Fig. S9 Li 1s XPS spectra for (a) Li_2S_6 and (b) Fe-CS after adsorption test.

Fig. S9 revealed that the Li 1s spectra for Li_2S_6 contained one peak at 55.4 eV, corresponding to Li-S bond. After adsorption test, an extra peak with a higher binding energy of 55.9 eV appeared which was caused by the bonding of Li to N and O.^[3,4]

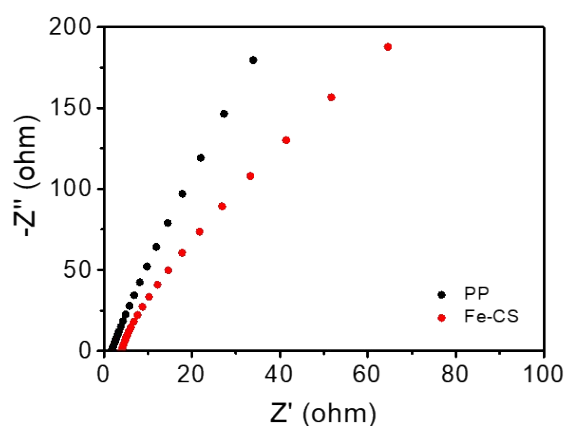


Fig. S10 EIS plots of Fe-CS/CB-modified separators and PP separators.

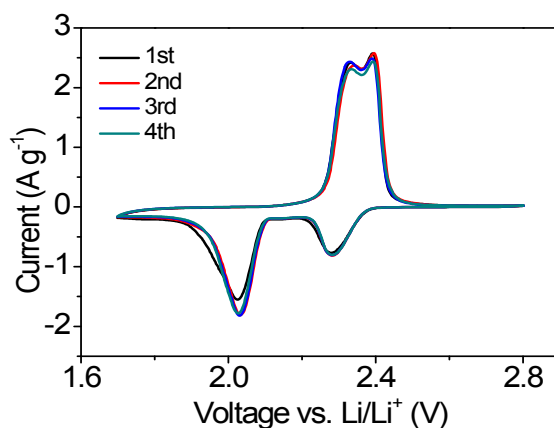


Figure S11. CV curves of the cell with Fe-CS/CB modified separator in the first four cycles.

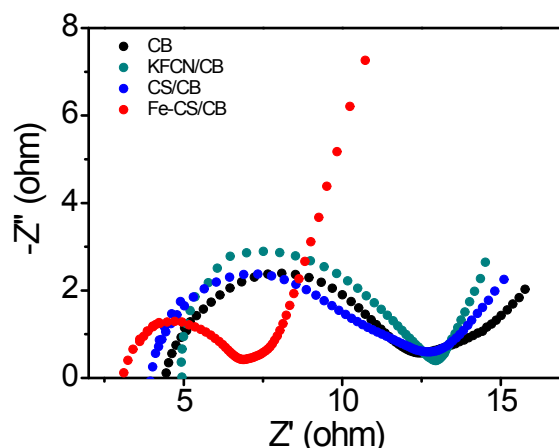


Fig. S12 EIS plots of cells with KFCN, CS, CB and Fe-CS modified separators after 30 cycles.

According to the literature^[5], the reduction of EIS plots of cells after 30 cycles in Fig. S12 compared with the fresh cells in Fig. 4d is mainly caused by the consumption of sulfur during cycling, making for a better interphase electronic contact between particles. The smaller semicircle of the cell with Fe-CS modified separator is most likely related to the better accessibility of active material and less formation of non-conductive Li_2S , resulting in the excellent capability of polysulfide conversion in Fe-CS aerogel.^[6]

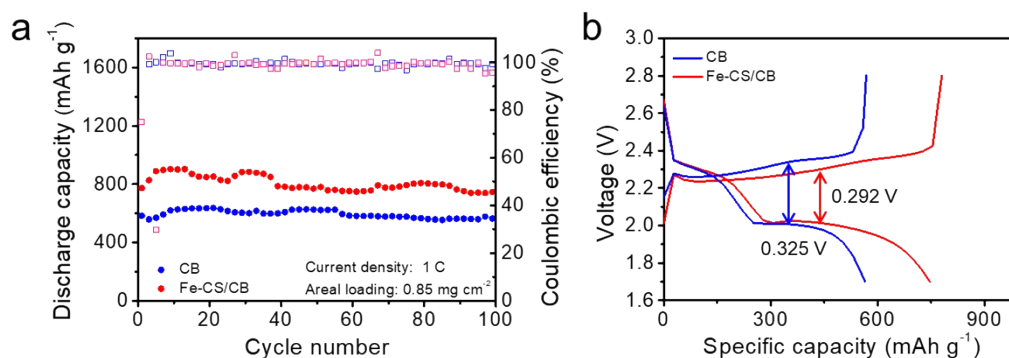


Fig. S13 (a) Cycling performance the cells with CB and Fe-CS/CB cathode at 1 C. (b) Discharge–charge profiles after 100 cycles.

The common cathode was prepared by mixing the sulfur (50 wt %), carbon black (40 wt %) and PVDF (10 wt %), and the cathode with aerogel was prepared by mixing the sulfur (50 wt %), carbon black (35 wt %), aerogel (5 wt %) and PVDF (10 wt %). The separators were unmodified PP separators. As exhibited in Figure S13, the cathode with aerogel delivers a discharge capacity of 747 mA h g^{-1} and a polarization of 0.292 V after 100 cycles at 1 C. As a comparison, the common cathode has a lower discharge capacity of 564 mA h g^{-1} and a higher polarization of 0.325 V , indicating that the incorporation of aerogels into the cathode can improve the sulfur utilization and redox reaction kinetics by trapping polysulfide and catalyst effect.^[7]

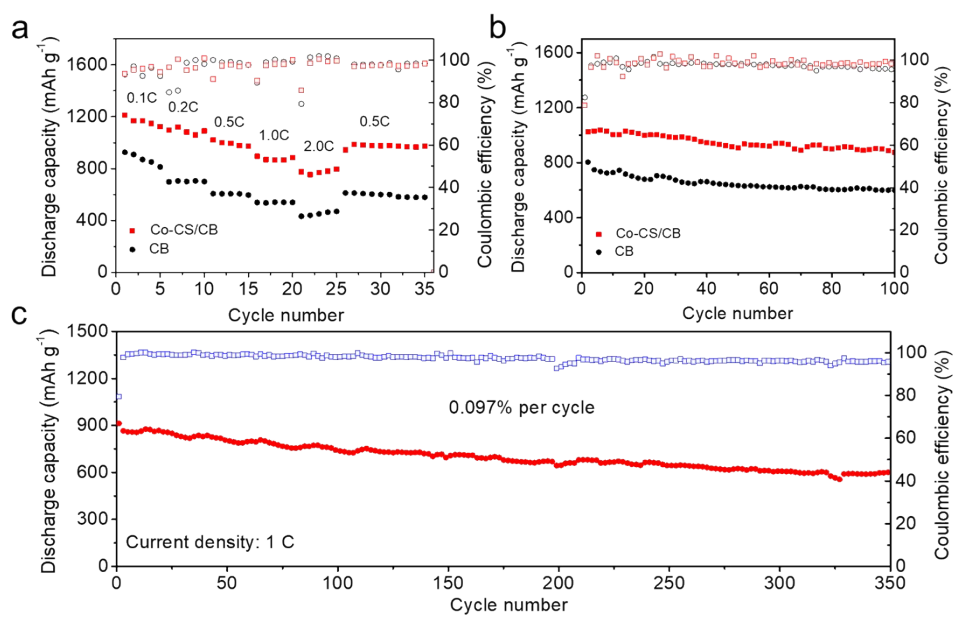


Fig. S14 Electrochemical properties of Li-S cells with Co-CS/CB modified separators. (a) Rate capability. (b) Cycling performance at 0.5 C. (c) Long-term cycling performance at 1 C.

Table S1. Comparison of the performance of our separator in Li-S batteries with selected state-of-the-art modified separators.

Modified separator	Initial capacity (mA h g ⁻¹)	Rate performance	Areal capacity for high sulfur loading (mA h cm ⁻²)	Cyclic decay rate	Ref.
Fe-CS/CB-PP separator	1324 (0.1 C)	882 ^a mA h g ⁻¹ (2 C)	7.68 for 8.14 mg cm ⁻² (0.2 C)	0.069 % (500 cycles at 1 C)	Our work
B/2D MOF-Co separator	1138 (0.1 C)	590 mA h g ⁻¹ (2 C)	7.8 for 7.8 mg cm ⁻² (0.1 C)	0.07 % (600 cycles at 1 C)	Adv. Mater. 2020, 32, 1906722
PIN-PP separator	1036 (0.1 C)	668 mA h g ⁻¹ (0.5 C)	4.14 for 4 mg cm ⁻² (0.1 C)	0.09 % (200 cycles at 0.2 C)	Adv. Energy Mater. 2020, 10, 1902872
(LDH/GO) ₂₀ separator	1334 (0.1 C)	654 mA h g ⁻¹ (2 C)	4.8 for 4 mg cm ⁻² (0.1 C)	0.08 % (500 cycles at 0.2 C)	J. Mater. Chem. A, 2020, 8, 1896-1903
Li-CON@GN/Celgard separator	1371 (0.1 C)	~800 mA h g ⁻¹ (2 C)	~3.2 for ~2 mg cm ⁻² (0.1 C)	0.057 % (600 cycles at 1 C)	Energy Storage Mater. 2020, 29, 207-215
S ₆ ²⁻ -VPP separator	1310 (0.1 C)	~900 mA h g ⁻¹ (2 C)	1.3 for 1 mg cm ⁻² (0.1 C)	0.082 % (300 cycles at 0.2 C)	Angew. Chem. 2019, 131, 11900-11904
p-carbon-coated p-separator	1204 (0.2 C)	539 mA h g ⁻¹ (2 C)	–	0.33 % (100 cycles at 0.2 C)	J. Mater. Chem. A, 2019, 7, 3772-3782
a-Ti ₃ C ₂ -S/d-Ti ₃ C ₂ /PP	1062 (0.2 C)	513 mA h g ⁻¹ (2 C)	~1.1 for 1 mg cm ⁻² (0.2 C)	0.25 % (200 cycles at 2 C)	ACS Nano 2018, 12, 2381-2388

^a The mean and standard deviation are 859 and 13.

References

- [S1] H. J. Peng, G. Zhang, X. Chen, Z. W. Zhang, W. T. Xu, J. Q. Huang, Q. Zhang, *Angew. Chem. Int. Ed.*, 2016, **55**, 12990.
- [S2] X. F. Liu, H. Chen, R. Wang, S. Q. Zang, T. C. W. Mak, *Small* 2020, 2002932.
- [S3] Y. K. Wang, R. F. Zhang, J. Chen, H. Wu, S. Y. Lu, K. Wang, H. L. Li, C. J. Harris, K. Xi, R. V. Kumar, S. J. Ding, *Adv. Energy Mater.*, 2019, **9**, 1900953.
- [S4] Z. W. Seh, H. Wang, P. C. Hsu, Q. Zhang, W. Li, G. Zheng, H. Yao, Y. Cui, *Energy Environ. Sci.*, 2014, **7**, 672.
- [S5] Z. Deng, Z. Zhang, Y. Lai, J. Liu, J. Li, Y. Liu, *J Electrochem. Soc.*, 2013, **160**, A553-A558.
- [S6] N. A. Cañas, K. Hirose, B. Pascucci, N. Wagner, K. A. Friedrich, R. Hiesgen, *Electrochim Acta*, 2013, **97**, 42-51.
- [S7] Z. L. Xu, S. Lin, N. Onofrio, L. Zhou, F. Shi, W. Lu, K. Kang, Q. Zhang, S. P. Lau, *Nat. Commun.*, 2018, **9**, 4164.